Jets in $d(p)$-A collisions: Color transparency or energy conservation

Michael Kordell II and Abhijit Majumder
Department of Physics and Astronomy, Wayne State University, Detroit, Michigan 48201, USA

(Received 23 February 2016; revised manuscript received 21 March 2018; published 11 May 2018)

The production of jets, and high momentum hadrons from jets, produced in deuteron-Au (d-Au) collisions at the BNL Relativistic Heavy Ion Collider (RHIC) and proton-Pb (p-Pb) collisions at the CERN Large Hadron Collider (LHC) are studied as a function of *centrality*, a measure of the impact parameter of the collision. A modified version of the event generator PYTHIA, widely used to simulate p-p collisions, is used in conjunction with a nuclear Monte Carlo event generator which simulates the locations of the nucleons within a large nucleus. We demonstrate how events with a hard jet may be simulated, in such a way that the parton distribution function of the projectile is "frozen" during its interaction with the extended nucleus. Using our approach, we demonstrate that the puzzling enhancement seen in peripheral events at RHIC and the LHC, as well as the suppression seen in central events at the LHC, are possibly due to *mis*-binning of central and semicentral events, containing a jet, as peripheral events. This occurs due to the suppression of soft particle production away from the jet, caused by the depletion of energy available in a nucleon of the deuteron (in d-Au at RHIC) or in the proton (in p-Pb at LHC), after the production of a hard jet. We conclude that partonic correlations built out of simple energy conservation are responsible for such an effect, though these are sampled at the hard scale of jet production and, as such, represent smaller states.

DOI: 10.1103/PhysRevC.97.054904

I. INTRODUCTION

In the context of hard processes in heavy-ion collisions, maximally asymmetric collisions, such as d-Au at the BNL Relativistic Heavy Ion Collider (RHIC) and p-Pb at the CERN Large Hadron Collider (LHC), have served the purpose of baseline measurements: quantifying initial state nuclear effects without the presence of a hot and dense extended final state. Early measurements of suppressed back-to-back hadron correlations, with momenta perpendicular to the colliding nuclei, at the STAR detector at RHIC [1,2] for Au-Au collisions, compared with a null effect in d-Au (compared with p-p) established jet quenching as a final state effect that takes place primarily in the presence of an extended quark-gluon-plasma (QGP). These jets, with momentum transverse to the incoming beams, were quenched in Au-Au, but were minimally affected in d-Au collisions.

These were consistent with measurements of a lack of suppression in the expected yield of high transverse momentum (leading) hadrons in d-Au collisions at both the STAR [2] and PHENIX [3] detectors. In 2006, the PHENIX Collaboration extended this analysis to centrality (the experimental measure of impact parameter) dependent suppression [4,5]. These data demonstrated an odd enhancement in the yield of high momentum hadrons in peripheral d-Au events. While nuclear effects which modify the dynamics of jet production were expected in central events, where nucleons from the deuteron encounter several collisions with the large nucleus, these were not expected at all in peripheral events where the deuteron has fewer collisions with the large nucleus.

Recently, there have been a series of new measurements, both by PHENIX [5] at RHIC and by ATLAS at the Large Hadron Collider (LHC), on the spectrum of high transverse momentum (high-p_T) jets produced in d-Au [6] and p-Pb [7] collisions. The measurements plot the centrality dependent nuclear modification factor R_{dAu} of high-p_T jets: a ratio of the detected yield of jets to that expected based on an estimate of the number of nucleon-nucleon collisions in one $p(d)$-A collision. In both cases, one notices an enhancement in the R_{dAu} in peripheral events and a "suppression" in central collisions. In a study of the rapidity dependence of the reconstructed jet, by the ATLAS Collaboration, it was observed that this peripheral enhancement and central suppression was much more prevalent in the p-going direction and vanishing in the Pb direction.

These results are rather counterintuitive. Nuclear effects, in particular those that involve jets and jet production, are expected to be dominant in central events where the initial state engenders several nucleon-nucleon collisions; also, the final outgoing partons have to traverse a more extended medium. Similar arguments may be ascribed to the rapidity dependence of hard particle production, with hard partons traversing longer distances in the nucleus-going direction than in the p- or d-going direction.

In this paper, we posit that events which lead to the production of a hard jet, requiring an initial state parton with a considerable value of x, have initial states with fewer soft partons, due to the large amount of energy that has been drawn away from the nucleon by the high-x parton. This effect is most pronounced on the partons in the $p(d)$-going direction, and much less on the A-going direction as the formation of a hard parton in a single nucleon (in a nucleus) does not effect the soft parton distribution in the remaining nucleons. The higher the x required, the greater the suppression is in

the soft particle production. Thus reactions with very high energy jet production probe the correlation between partons within a nucleon. This sensitivity to multiparton hard-soft correlations is unique to these experiments, which probe a hitherto unmeasured facet of nucleon structure: Is there a strong correlation between the x values of the leading partons in a given event and the total number of partons in the nucleon in that event? By "strong" we are suggesting something more than the trivial correlation due to straightforward energy conservation: Is there a kind of *color transparency* in the initial state, for events with a hard jet in the final state? Our calculations do not provide a clear answer to this second question. Beyond this, another goal of this work is to provide a reliable event generator, without any new tunable parameters, which may be used, with certain caveats, to reproduce at least some portion of these new data on $p(d)$-A collisions with jet production (While we have introduced shadowing corrections on the parton distribution functions, the parameters of the shadowing were fixed in Ref. [8]). The results of this paper will provide detailed input to a more dedicated event generator that will have to be constructed to study such collisions in greater detail.

In the remainder of this paper, we describe our model and how soft particle production is affected by the production of a hard jet. To make direct connection to experiments, we set out to modify the PYTHIA event generator [9] which is used extensively to model p-p collisions. To date there have been several approaches which have attempted to describe this new striking physics result. In Ref. [10], the authors proposed a similar mechanism of enhancement in peripheral events and suppression in central events but did not incorporate it in an event generator framework. In Ref. [11], the authors proposed that the wave function of the proton is considerably modified in the presence of a hard parton. In Ref. [12], the authors attempted to understand the effect of the energy depletion due to jet formation using the HIJING event generator [13,14]. In none of these calculations could the authors achieve widespread agreement with the data. The current effort has been constructed entirely within the PYTHIA event generator, by modifying it. As such, we suffer from several constraints which are inbuilt within this particular event generator. The reader may question why we did not use the HIJING event generator as in Ref. [12]. The primary reason behind this is the resampling of the parton distribution function between collisions; this has the effect of the proton (or nucleon in d-Au collisions) changing its parton distribution function between successive collisions which changes the distribution of soft partons that arise after the hard parton has been extracted.

In the subsequent section we describe the event generator that samples the location of the nucleons in the two incoming nuclei. In Sec. III, we outline the changes introduced into the PYTHIA event generator. In Sec. IV we present comparisons with experimental data at RHIC and LHC. Our conclusions are presented in Sec. V.

II. SAMPLING THE NUCLEAR DISTRIBUTION

Maximally asymmetric collisions such as p-Pb or d-Au represent cases where the experimentally determined centrality of the event appears to be influenced by the production of a hard jet. In order to simulate jet production in such systems, the PYTHIA event generator was modified and extensively used. This modification of the event generator depended on the number of nucleon-nucleon collisions in a given $p(d)$-A event. This number of collisions was determined using several methods. In this section we describe these methods.

Along with a description of our setup, we will explore and eliminate the most naive explanation of the observed correlation between jet production and centrality: The deuteron, due to its large size, often has the proton and neutron far apart, and thus cases where a jet is most likely to be produced, when either nucleon strikes the densest part of the oncoming nucleus, may coincide with cases where the other nucleon simply escapes without interaction leading to reduced soft particle production. It should be pointed out, in passing, that such a scenario is immediately ruled out by an almost identical correlation between jet production and centrality in LHC collisions, where there is only one proton colliding with the large nucleus.

A. The deuteron

Collisions at the LHC always involve a proton colliding with a Pb nucleus. However, at top RHIC energies the collisions are usually that of a deuteron (d) on a Au nucleus. The deuteron is an extremely well studied state in low energy nuclear physics. The wave function of the deuteron is given by the Hulthén form [15]:

$$\psi_H(r) = \frac{e^{-ar} - e^{-br}}{r}, \tag{1}$$

where $a = 0.228/\text{fm}$, $b = 1.18/\text{fm}$. The probability distribution of a nucleon within a deuteron is given as

$$\rho(r) = |\psi_H(r)|^2. \tag{2}$$

This distribution is sampled to obtain the positions of the two nucleons.

As is well known, the Hulthén wave function leads to a rather wide nuclear distribution. This is illustrated in Fig. 1,

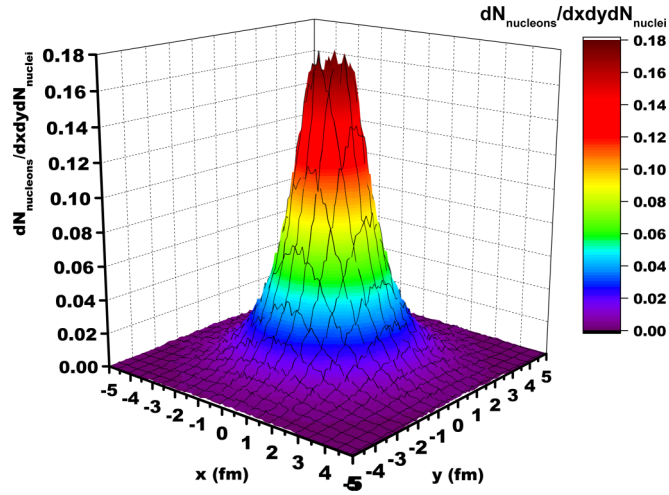

FIG. 1. The sampled Hulthén distribution for two nucleons in a deuteron.

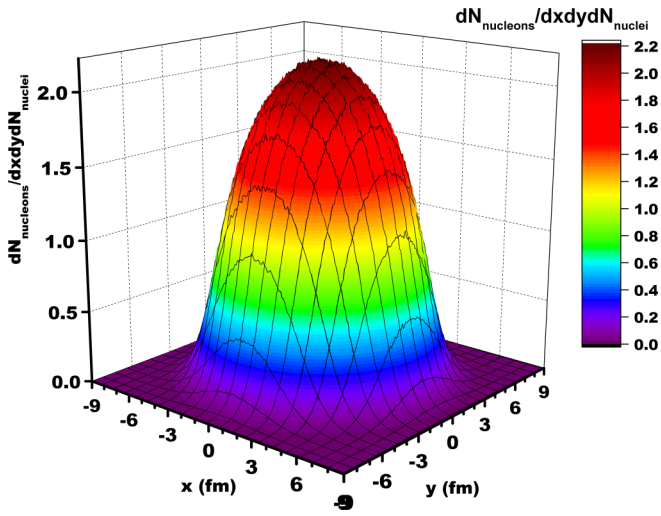

FIG. 2. The sampled Woods-Saxon distribution for a large nucleus (in this case Au with an $A = 192$.)

where we plot three representative events, with both the Au nucleus and the deuteron distributions projected on the z axis, which is the axis of momentum of the two nuclei. As can be seen from Fig. 1 the nucleons in the deuteron may be close together, as well as a gold radius apart. Due to the large separation between the nucleons, excluded volume corrections were unnecessary but were still included.

B. The large nucleus (Au or Pb)

Moving to the nuclear state, there are several methods that may be used to simulate the fluctuating initial state represented by the large nucleus. In this work, we will only focus on the Au or Pb nucleus, as these are studied experimentally. In most cases, we will use the Woods-Saxon density distribution, given at a radial distance r as

$$\rho(r) = \frac{\rho_0}{1 + e^{(r-R)/a}}, \tag{3}$$

where ρ_0 is a constant related to the density at the center of the nucleus, R is the radius of the nucleus, and a is the skin depth. These parameters are chosen to match those used by the experiments at RHIC and LHC (for Au, $a = 0.535$ fm, $R = 6.38$ fm; for Pb, $a = 0.546$ fm, $R = 6.62$ fm). The Woods-Saxon distribution of Eq. (3) is a single-particle distribution. On top of this we introduce a nucleon-nucleon correlation by hand: the excluded volume correction. This is done similar to the method of Ref. [16], where we generate a set of three random numbers which isolate the location of a nucleon. If this location is within an exclusion distance of $d = 2R_p$ (twice the proton radius) of another nucleon, then this location is abandoned and another generated. The process is continued until all A nucleons have been included. At the end of this process the center of mass of the nucleus is calculated and the nucleus is recentered. The average sampled distribution for Au generated via this process is given in Fig. 2.

While only the Hulthén form is used for the deuteron, several probability distributions beyond Woods-Saxon were tried for the nucleon distribution in a large nucleus. These include distributions based on shell-model wave-functions both with and without a modified delta interaction to account for the short range repulsion between nucleons in a nucleus [17] (simple excluded volume). However, none of these enhancements led to any noticeable changes in the final results as compared to the Woods-Saxon distribution with a simple excluded volume. It should be pointed out that in this effort we have only considered p-A and d-A, collisions which only sample the single- and two-nucleon distribution within a nucleus. It is entirely possible that the collision of nuclei larger than a deuterium with nuclei smaller than Au may lead to the greater role for multiparticle correlations within a nucleus. There is very little information in nuclear structure on such multiparticle correlations. We will not discuss this issue further in this effort, and only focus on simulations using the Woods-Saxon distribution with an excluded volume.

C. Transverse Size of nucleons and binary collisions

The nuclear Monte Carlo generator samples nucleons from the Au (or Pb) side and from the d side and then projects these on the x-y, plane as shown in Fig. 3. In the work presented in this paper, the transverse size of the nucleons has not been modified with the energy of the collision. The inelastic cross section for nucleon-nucleon scattering is known to grow with collision energy. While centrality selection at the nuclear level is one of the major issues dealt with in this effort, no centrality selection is imposed on the individual nucleon-nucleon encounters. As a result, when a proton from the d overlaps with another from the Au side, no matter how small the overlap, the entire parton distribution function (PDF) of either nucleon is enacted in the collision; i.e., nucleon-nucleon collisions are not expected to have any centrality dependence. In a future effort, an impact parameter in nucleon-nucleon collisions will be used to generate particle production in events where the two nucleons do not overlap completely.

Glancing at Fig. 3, it becomes clear that if the transverse size of the nucleons is increased with increasing energy then this will lead to an increase in the number of binary collisions, and that will lead to an artificial excess enhancement of the particle production from each individual nucleon-nucleon collision. In this work, we will use the event generator PYTHIA to simulate nucleon-nucleon collision. Within the PYTHIA event generator the cross section increases with energy. To counter the possible artificial increase in particle production with energy, the full cross section generated by PYTHIA is used with no change in the geometric size of the nucleon with the energy of the nuclear collision.

Once both nuclei have been generated, and centers of mass determined, the impact parameter b is simulated with a probability distribution $dP/db^2 = 1/b_{\rm Max}^2$, and the angle of the impact parameter is determined randomly between 0 and 2π. The maximal impact parameter $b_{\rm Max}$ is chosen such that no dependence is observed in minor changes of this quantity: We pick a value of $b_{\rm Max}$, then run millions of events with $0 < b < b_{\rm Max}$ chosen at random and count the total number of collisions. Then we pick a larger value of $b_{\rm Max}$, and repeat the process until the total number of collisions stops increasing. Increasing $b_{\rm Max}$ beyond this value has no further effect, and

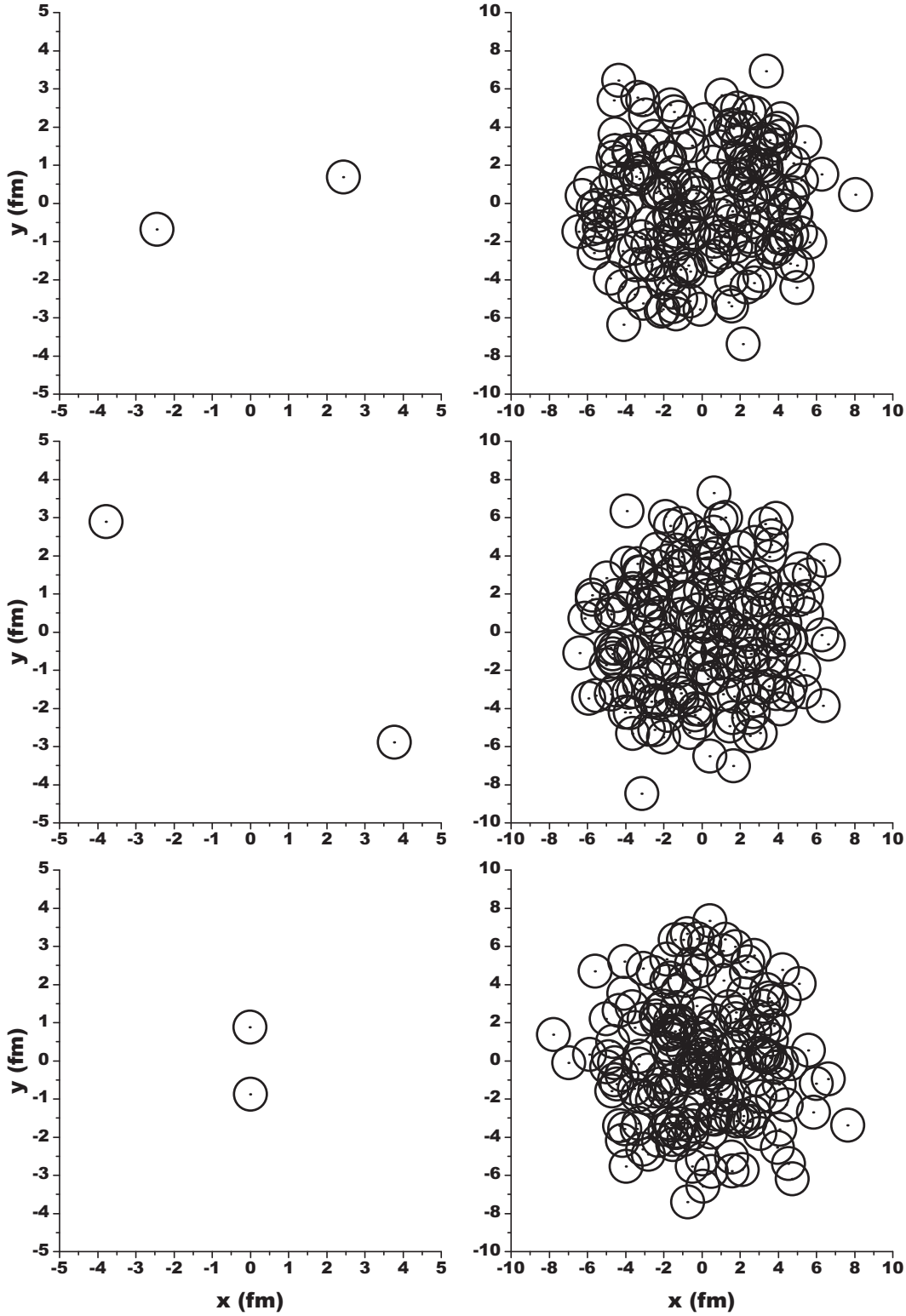

FIG. 3. Three separate events in d-Au collisions. Nucleon distributions are projected onto the x-y plane.

this determines the value of b_{Max} used in the remainder of the simulation. There is no further reorienting of the nuclei. The number of binary collisions can now be determined by simply counting the number of nucleons in the Au side, whose centers are within a transverse distance $d = 2R_p$ of a nucleon in the deuteron. There arise events where not a single collision takes place; these events are dropped from the analysis.

Based on the above considerations, we present the results of the nuclear Monte Carlo simulations for a d-Au collisions in

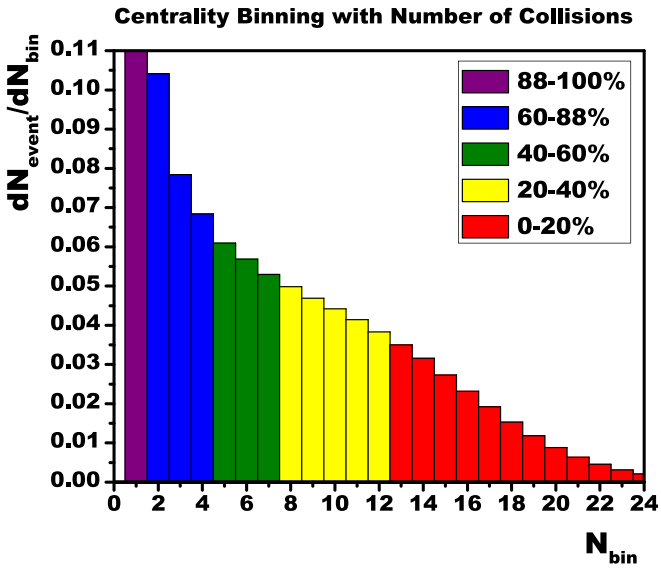

FIG. 4. The event distribution in d-Au collisions as a function of the number of binary collisions.

Fig. 4. In Fig. 4, the distribution of events as a function of the number of binary collisions is presented. Following this, events are divided into four bins (0–20%, 20–40%, 40–60%, 60–88%) based on the fraction of the total number of events contained in these bins. These bins also correspond to the bins used by the PHENIX experiment. Each of these bins in the number of collisions represents a range of overlapping impact parameters. While this represents the standard method of determining centrality in theoretical calculations or simulations, we will show, in a later section, that this method of determining the centrality of the event leads to results that are not consistent with experimental results for high transverse momentum (high-p_T) pion, charged particle, and jet production at both RHIC and LHC energies.

In this section we have focused mostly on d-Au collisions where both incoming nuclei have to be simulated. In subsequent sections we will also present results for p-Pb collisions where only one nucleus needs to be simulated. There are no other considerations concerning p-Pb that need to be made other than the location of the p is set by the impact parameter b. As pointed out above, no explicit change in the transverse size with energy has been used in this first attempt to understand the behavior of jets in $p(d)$-A collisions. We also mention that, in all simulations, we keep track of the isospin of the nucleons.

III. THE MODIFIED PARTON DISTRIBUTION FUNCTION

Using the nuclear collision event generator, the number of nucleon-nucleon collisions in each event may be determined. Each nucleon in the deuteron, in a d-Au collision at RHIC, or the proton in p-Pb collisions at the LHC, will potentially engender several collisions with nucleons in the large nucleus. At RHIC the relativistic γ factor is about a 100 while it is close to 2750 at the LHC. In the rest frame of a nucleon, its internal partonic structure is continuously fluctuating. For a fluctuation at an energy scale Q, the timescale is given by Heisenberg uncertainty as $\delta\tau \sim 1/Q$. However, when it is boosted by a gamma factor of $\gamma \sim E/m_n$ (m_n is mass of the nucleon and E is its energy in the lab frame), the fluctuation lives for a time $\delta t \sim E/(m_n Q)$.

In order to get a feeling for this effect, we take the extreme case of of a very high Q^2 fluctuation which leads to jet production. For the specific case where the jet originates from a parton that takes 1/3 of the energy of the nucleon, the lifetime of these fluctuations is $3/m_n \sim 0.6$ fm/c. Within this time, the nucleon has moved a distance of $c\delta t = 0.6$ fm in the laboratory frame. This is the mean distance that a nucleon can travel with a given high Q^2 parton configuration unchanged. We refer to this as a configuration distance (a distance over which the parton distribution can be considered to be frozen). After the configuration distance has been traversed, the nucleon will fluctuate to another configuration which will have its own lifetime and configuration distance. The oncoming nucleus has a diameter of $2R_A \sim 12$ fm. In the laboratory frame this is contracted to a distance $d = 2R_A/\gamma$. At RHIC, $\gamma = 100$, thus the nuclear diameter is contracted to a distance of 0.12 fm. Thus a nucleon which has fluctuated to a high Q^2 configuration with a few hard partons will be able to traverse the entire oncoming nucleus within the lifetime of the configuration. Alternatively stated, the configuration distance far exceeds the contracted length of the entire nucleus.

As a result of this time dilation effect, the parton distribution of the nucleons in deuteron (in a d-Au) collision, or that in the proton in p-Pb collisions, is "static" (frozen) as it progresses through the large nucleus. We use the word static to indicate that the parton distribution, though being continuously depleted by collisions with partons in the nucleons from the large nucleus, is itself not undergoing any intrinsic fluctuation in the course of its passage through the large nucleus. On the opposing side, only one of the nucleons in the nucleus will fluctuate to a configuration with hard partons, to produce a jet pair. However, since the projectile nucleon has a static parton distribution function (PDF) in the course of the multiple collisions, one treats the entire line of struck nucleons as a single "super"-nucleon.

This brings the discussion to the primary point of this paper: Consider the case where, in the course of fluctuations of the PDF, the proton in p-Pb (or one of the nucleons in d-Au) has focused a large amount of energy within a single parton. This parton, in collision with a similar parton in the oncoming nucleus, will produce back-to-back jets at mid-rapidity. The presence of a parton with such a large energy will lead to less energy being available for the production of other softer partons. It is also possible that the entire nucleon has fluctuated to a state with a few partons. As a result, there will be a depletion in the number of soft partons in the proton in p-Pb (or projectile nucleon in d-Au) collisions. A similar situation will occur in one of the nucleons within the large nucleus. As a result, an event with a jet will lead to the production of fewer charged particles.

To simulate this effect, we treat the collision of the p (or any of the nucleons in d) with a string of n nucleons in the large nucleus as a single collision between a nucleon and an object with a larger (modified) PDF. As a result, the PDF of both the projectile nucleon and target is sampled only once. To be clear, there are several methods to carry this out; we will only

focus on the most expeditious method. In the remainder of this paper, we will refer to the collection of n nucleons struck as a single entity by the projectile nucleon as a "super"-nucleon. Resampling the PDF of the projectile nucleon will change the PDF; this will destroy the correlation between hard jet and soft particle production.

We are now going to simulate a $p(d)$-A collision as a modified p-p collision in the PYTHIA event generator. For the case of p-A, we refer to one of the nucleons as the projectile and leave its PDF unchanged. The target nucleon will be modified into a super-nucleon. As a first step to simulate the super-nucleon (which represents the entire line of nucleons struck by the projectile in a large nucleus), we enhance the PDF of the incoming target nucleon as

$$f^{E,S}(x) = n_P f^P(x) + n_N f^N(x). \tag{4}$$

Here $n_P(x)$ is the parton distribution function (for any parton) within an isolated proton, $f^N(x)$ is that for a neutron, and n_P and n_N are the numbers of protons and neutrons struck by the projectile nucleon. The PDF of the projectile nucleon is unchanged. Along with this the energy of the super-nucleon is also enhanced as $E_S = (n_P + n_N)E$, where E is the energy of the projectile nucleon in the laboratory frame. This leads to an energy and number modified PDF for a super-nucleon as

$$\begin{aligned} f^{E,S}(x_S) &= n_P f^P(x_S) + n_N f^N(x_S) \\ &= n_P f^P(x/n) + n_N f^N(x/n). \end{aligned} \tag{5}$$

This prescription turns out to produce a very faithful description of the soft particle production in d-Au (or p-Pb) collisions. This is illustrated by the increase in the yield of soft particles with increasing enhancement of the super-proton shown in Fig. 5. One notes both an increase in the mean value of charged particle production as well as an increase in the event-by-event fluctuation in charged particle production, as expected.

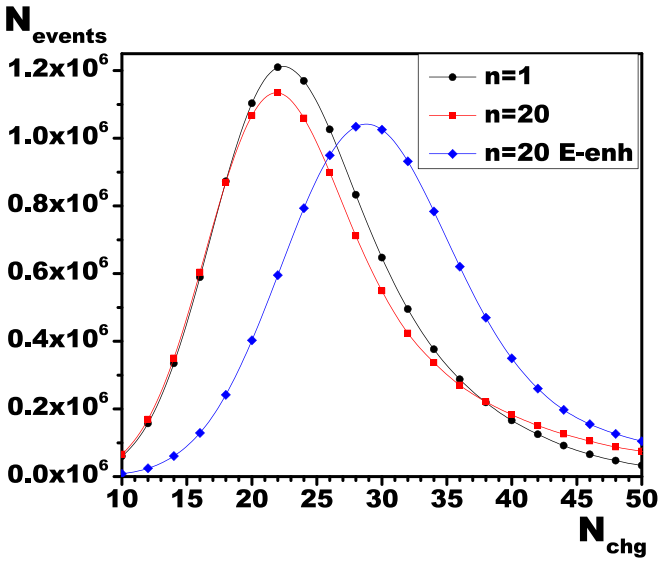

FIG. 5. The multiplicity of charged particles in a simulated d-Au collision with the Au side simulated as a super-nucleon with a parton distribution function given as $f^{E,S}(x_S) = n_P f^P(x_S) + n_N f^N(x_S)$, and energy enhanced as $E_S = (n_P + n_N)E$ [and corresponding momentum fraction $x_S = x/(n_N + n_P)$]. In the above plot $n_P = 10$ and $n_N = 10$.

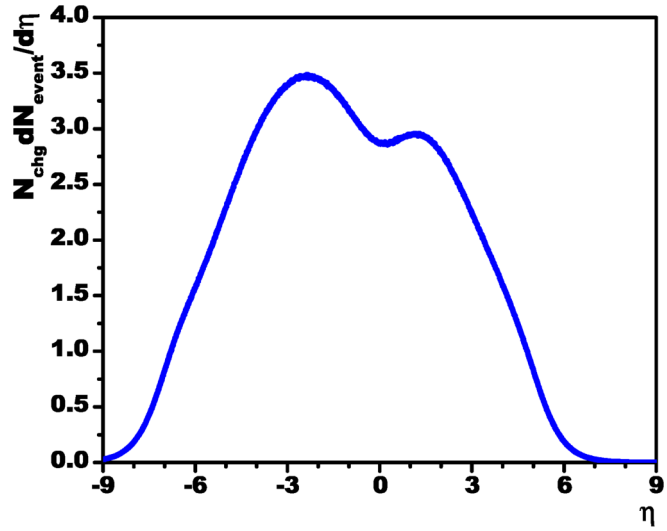

FIG. 6. The pseudorapidity distribution of charged particles in a simulated d-Au collision with the Au side simulated as a super-nucleon with a parton distribution function given as $f^{E,S}(x) = n_P f^P(x) + n_N f^N(x)$ and energy enhanced as $E_S = (n_P + n_N)E$.

Yet another feature of this formula for the super-nucleon is that it also gives a rather faithful representation of the pseudorapidity distribution of the produced charged particles. This distribution for minimum bias events, plotted in Fig. 6, shows the "classic" asymmetric double humped structure of the pseudorapidity distribution for d-Au collisions at RHIC energies. The overall normalization is less than that measured in actual experiments. However, one should recall that we are generating this by modifying PYTHIA such that only the interactions between the projectile nucleon and the column of struck nucleons are included. No re-interaction of the produced particles with the remainder of the nucleus is included, and this leads to an obvious depletion in overall particle production. The assumption being made in comparing these results to experimental data is that even though the overall number of charged particles (or transverse energy) produced is not matched between the simulations and the experiment, the relative distribution between centrality bins will be the same as in the experiment.

In spite of the success in soft particle production using the prescription of enhancing both the PDF and the the energy of a nucleon in the target nucleus, this procedure leads to an uncontrollable modification to the high momentum (large-x) portion of the PDF (see Fig. 7). This is to be expected, as the super-nucleon now has $n = n_P + n_N$ times the energy of a single nucleon, and can thus produce hard partons of higher energy (higher even than the kinematic bound of 100 GeV at RHIC, or 2.75 TeV at the LHC) without the penalty of a rapidly falling PDF. As an illustration of this effect, we plot the ratio of a gluon spectrum from a super-nucleon to that from a regular nucleon as a function of the ratio of the energy of the gluon to that of the projectile nucleon (un-enhanced nucleon). Consider a parton with energy E_p produced from a super-nucleon with

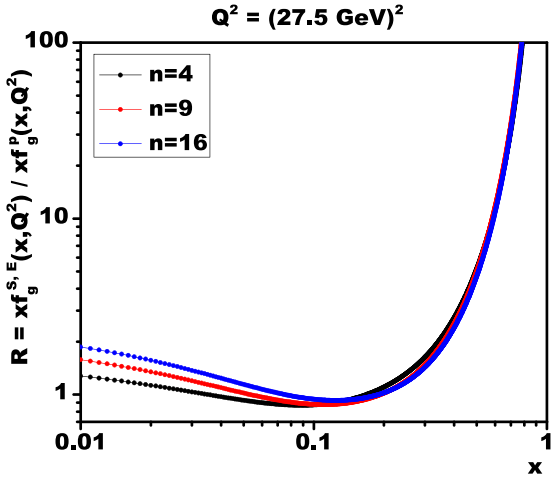

FIG. 7. The ratio of the gluon distribution in a super-nucleon (where both the energy and PDF are enhanced) to that in a nucleon as a function of x, the energy fraction of the gluon: $f^{E,S}(x_S)/f^P(x)$, where $x_S = x/n$ and n is the number of nucleon nucleon collisions. See Eqs. (4) and (5) and the discussion following them.

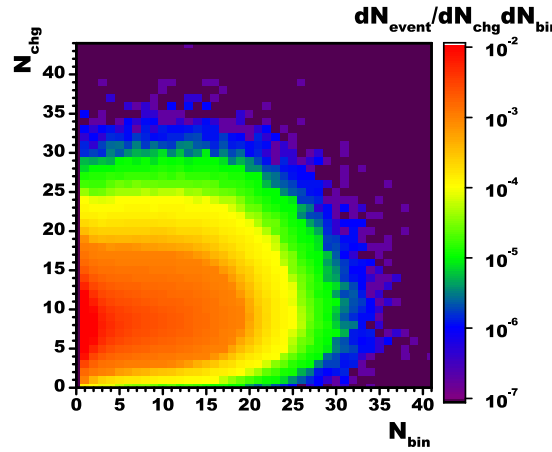

FIG. 8. The correlation between number of binary nucleon-nucleon collisions $N_{\rm bin}$ and the produced number of charged particles produced $N_{\rm chg}$ in the absence of energy enhancement in a p-Pb collision at LHC energies. One notes an increase of the mean $N_{\rm chg}$ with $N_{\rm bin}$, although it is not commensurate with experiment. The color contours represents the number of events that produce an outcome with a given $N_{\rm chg}$ and $N_{\rm bin}$ divided by the total number of events.

energy $(n_P + n_N)E$, where E is the energy of a single nucleon. Thus, for the super-nucleon, the fraction $x_S = x/(n_P + n_N)$, where x is the fraction E_p/E. The ratio of $f^{E,S}(x_S)/f^P(x)$ for a $Q^2 = 27.5$ GeV^2 is plotted in Fig. 7.

It is interesting to note that the soft gluon ($x < 0.1$) production is enhanced in the super-nucleon as a function of the total enhancement coefficient $n = n_P + n_N$. There is no enhancement for intermediate energy gluons $x \sim 0.1$, and then an almost n-independent enhancement for higher energy gluon with $x > 0.1$. Note that this will of course be broken as one moves past the $x \geqslant n$ point. However, since the denominator of the ratio plotted in Fig. 7 will vanish, this cannot be plotted in the manner of Fig. 7.

Due to this large enhancement in the hard portion of the PDF, this straightforward enhancement of the PDF for a super-nucleon cannot be used. Since the primary focus of the simulations reported in this paper has to do with jet production and its ensuing effect on soft particle production due to energy conservation, we will insist on keeping the jet production cross section as close to reality as possible, and not enhance the energy of the super-nucleon. This leads to a smaller increase in the number of charged particles produced as a function of the number of binary collisions. We present the correlation between the number of binary collisions, $N_{\rm bin}$ ($\equiv n$ for p-A), and the number of charge particles produced, $N_{\rm chg}$, in Fig. 8, in the absence of any energy enhancement of the super-nucleon. One notes a steady increase in the mean $N_{\rm chg}$ as a function of $N_{\rm bin}$, as the distributions get much more broad in $N_{\rm chg}$, although the increase is quantitatively less than that in the data.

For comparison with experiment, we will use a more complicated enhancement formula for the super-nucleon, where the soft portion of the PDF is modified by a shadowing function, and an enhancement by the number of collisions $n = n_P + n_N$, but no energy enhancement. We will use a shadowing function which modifies the super-nucleon PDF event by event, depending on the number of nucleons struck by the projectile nucleon. In the case of a d-Au collision, both nucleons may strike multiple nucleons and thus both collisions would be modeled as a nucleon super-nucleon collision. The shadowing formula used for this is given as

$$S(x) = 1 + [R(x) - 1]\frac{N_{\rm coll}}{\langle N_{\rm coll}\rangle}, \tag{6}$$

where $N_{\rm coll} \equiv n = n_P + n_N$ is the number of collisions with protons and neutrons encountered by a single projectile nucleon as it passes through the target nucleus in a given event. The mean number of collisions per projectile nucleon is given as $\langle N_{\rm coll}\rangle$. The shadowing factor of $R(x)$ which depends on x and the mass number of the target nucleus A, is taken from Ref. [8]. For the case of a quark it has the rather involved form

$$R_q^A = 1 + 1.19\ln^{1/6} A(x^3 - 1.2x^2 + 0.21x) - 0.1(A^{1/3} - 1)^{0.6}(1 - 3.5\sqrt{x}\,)\exp(-x^2/0.01). \tag{7}$$

In Fig. 9 we plot the change of the gluon shadowing function with respect to the number of collisions, $N_{\rm coll}$. As demonstrated in the plot, the PDF increases slightly, leading to the enhancement of the number of particles produced in the collision. The plots are normalized with an n-dependent constant C_n so that the momentum carried by the gluons in the proton remains the same, i.e.,

$$C_n \int_0^1 dx\, x R_g^A(x,n) f_g(x) = \int dx\, x f_g(x). \tag{8}$$

This constant is introduced for illustration purposes, to visually demonstrate the enhanced number of partons at $x \gtrsim 0.1$. In PYTHIA simulations (see Ref. [18] for details), a PDF is repeatedly sampled to obtain a series of forward momentum fractions x_i with $0 < i < N$. Strict energy conservation is

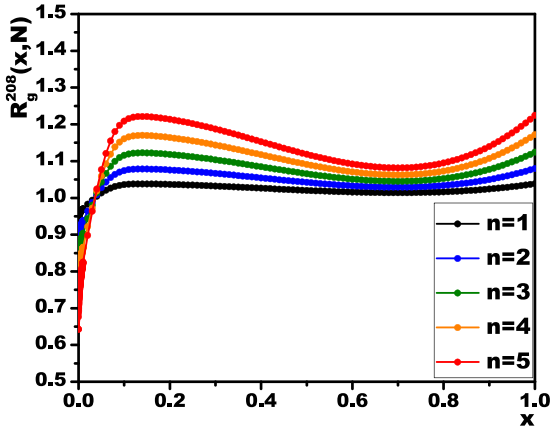

FIG. 9. The ratio of the shadowed gluon distribution in a super-nucleon to that in a regular nucleon as a function of the number of collisions $N_{\rm coll}$ [see Eq. (6)]. The normalization of each line is adjusted to reflect the function that is sampled by the PYTHIA event generator, which continues to sample distributions until the momentum of the nucleon is exhausted.

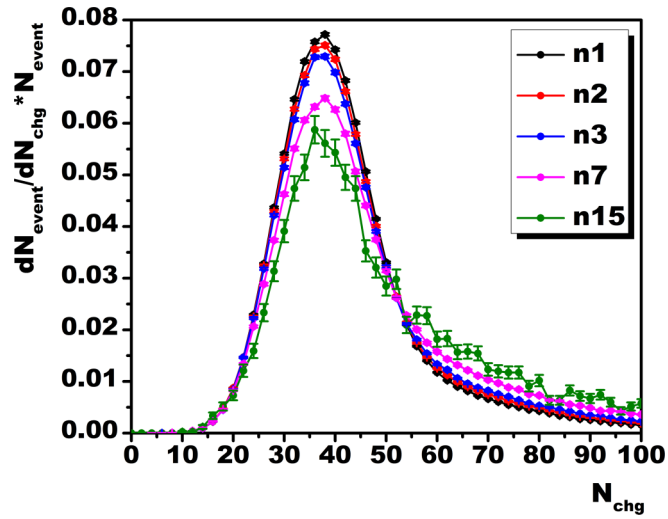

FIG. 10. The distribution of charged particles produced in a p-Pb collision, as a function of the number of collisions suffered by the projectile proton. For this plot the energy enhancement is removed.

enforced by sampling the PDF at the shifted fraction,

$$x_i' = \frac{x_i}{1 - \sum_{j=1}^{i-1} x_j}. \tag{9}$$

The process continues till $x_N' \to 1$, generating N partons. As a result, the numerical sampling is insensitive to any overall constants. However, the number of partons in a given momentum range is sensitive to any changes in the shape of the PDF. As a result, the samplings produce more partons at $x \gtrsim 0.1$.

The PYTHIA event generator has two sources of soft particle production: beam remnants and hard scattering. In this work, we modify the hard scattering component by introducing an $N_{\rm coll}$-dependent shadowing function [Eq. (6)]. This shadowing function enhances the number of hard partons sampled in the $x \gtrsim 0.1$ region. This increases the amount of multiparticle interactions. This leads to more particle production. We point out that the super-nucleon, in the remainder of this paper, has no enhancement in energy, and as a result the total energy of the partons sampled in the super nucleon equals the energy of one nucleon.

Without the enhancement in energy of the super-nucleon, one does not get the asymmetric distribution of produced charged particles as shown in Fig. 6. However, there is still an enhancement in the production of charged particles with increasing number of collisions, as shown in Fig. 8. While this is somewhat unphysical, our goal is to study the effect of energy conservation on the production of soft particles leading to centrality selection, in conjunction with a hard jet. The production of soft particles is illustrated for p-Pb collisions in Fig. 10, where the distribution of the number of charged particles per event is plotted for different number of collisions encountered by the proton. We present this plot for p-Pb at LHC energies. The effect of our modifications to the super-nucleon PDF has a smaller effect at these energies; the enhancement with increasing $N_{\rm coll}$ is larger at RHIC energies.

No doubt, this enhancement is proportionately less than that in Fig. 5; however, it is sufficient to allow us to bin by centrality. We point out once again that, in this process of simulating d-Au collisions at RHIC energies, or p-Pb collisions at LHC energies, the soft particle production is in no way commensurate with that in a real d-Au or p-Pb collision. We are carrying out this exercise to demonstrate the effect of a shift in centrality due to the production of a hard jet. We insist on the jet production cross section being unchanged in PYTHIA, while assuming that the reduced soft particle production in this model, as a function of the deduced centrality, is proportional to the particle production in a real collision.

To illustrate this issue, we plot the distribution of the number of events as a function of the number of produced charged particles in our simulations for d-Au collisions at RHIC energies in Fig. 11. As is clearly demonstrated by this figure, there are clear, nonvanishing ranges of particle production, which can be clearly demarcated as centrality bins. These simulations are all done using the *Hard-QCD* switch of PYTHIA. This is the case both for the particle production in general and for particle production in addition to the production of a hard jet. This is done so that the mechanisms that lead to soft particle production both in the presence and absence of a hard jet remain the same in the simulation.

In what follows, we will consider jet and leading hadron production at high-p_T and compare the effect of this on soft particle production. This will be done both for RHIC and LHC energies, for jet production at central rapidities. Charged particle detection, which leads to a centrality determination, will be carried out at all rapidities, i.e., over the entire collision. In actual experiments, charged particles are detected at rapidities far from where the jets are produced, in an effort to remove any correlation between the two processes. Since, in our simulated collisions, the number of particles produced is far fewer than an actual experiment, we collect charged particles at all rapidities, to allow to us distinguish between different centralities with higher statistics.

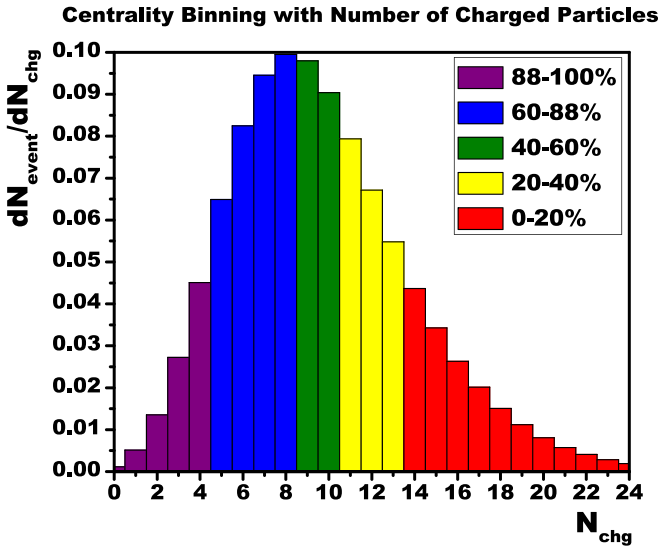

FIG. 11. The distribution of the number of charged particles produced and the division of the events in the four different centrality bins.

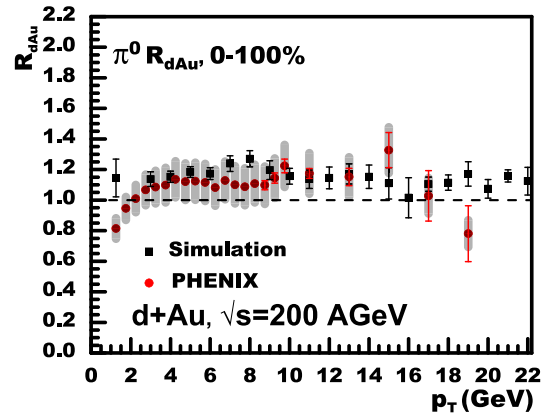

FIG. 12. The nuclear modification factor for neutral pions for minimum bias d-Au collisions at RHIC. Experimental data are taken from Ref. [19]

IV. COMPARISON WITH EXPERIMENT

In the proceeding sections, the model used to simulate jet (and high-p_T particle) production as a function of centrality, in d-Au collisions at RHIC and p-Pb collisions at the LHC, was described in detail. As stated before, our primary goal is twofold: to set up an event generator that may be used to faithfully represent the experimental data on hard soft correlations in asymmetric collisions, albeit with some caveats, as well as to understand the underlying cause of the startling results in such correlations using this new event generator.

Viewed in the laboratory or center-of-mass frame, it became clear that the nucleon PDF from both the projectile and the target are time dilated, and therefore cannot fluctuate in the short duration of the collision. This led us to abandon HIJING [13,14], and design a new event generator by modifying the PDF of one of the nucleons in a PYTHIA nucleon-nucleon collision. The effects of different modifications within PYTHIA and the overarching nuclear event generator were highlighted in the preceding sections. In the following, we demonstrate the successes and shortcomings of this new event generator when compared with actual experimental data.

The first comparisons are carried out for d-Au collisions at RHIC energies. These experimental results were also historically the first to show the odd effect of an enhancement in peripheral events and a mild suppression in central collisions. The data in question are the centrality, p_T, and rapidity (or pseudorapidity) dependent nuclear modification factor $R_{d\mathrm{Au}}$, defined as,

$$R_{d\mathrm{Au}} = \frac{\int_{b_{\min}}^{b_{\max}} d^2b \frac{d^4N_{d\mathrm{Au}}}{d^2p_T dy d^2b}}{\langle N_{\mathrm{bin}}(b_{\min},b_{\max})\rangle \frac{d^3N_{pp}}{d^2p_T dy}}, \tag{10}$$

where N denotes the yield of leading hadrons or jets, binned in transverse momentum and rapidity. In the numerator of the above formula, one also integrates over a range of impact parameter b, which in d-Au refers to the two-dimensional vector from the center of mass of the large nucleus to the center of mass of the deuteron (in Fig. 3 for example). The $\langle N_{\mathrm{bin}}(b_{\min},b_{\max})\rangle$ in the above formula refers to the mean number of binary nucleon-nucleon collisions per nuclear collision.

As a first step in studying the results of the current simulation in comparison with experimental data, we plot the nuclear modification factor for minimum bias collisions shown in Fig. 12. Here no division in centrality bins is carried out and thus there is no discussion of determining centrality by number of binary collisions or number of charged particles produced. This serves as a first test of the simulation, which performs extremely well in comparison to the data. The experimental data have been taken from Ref. [19]. Both the simulation and the experimental data show a similar trend: a p_T-independent, near lack of modification, with the possibility for a minor enhancement between 4 and 16 GeV. This is entirely to be expected: high energy jets are mostly unmodified in cold nuclear matter, and the minor enhancement can be attributed to the antishadowing peak (near $x \simeq 0.1$). We would further add that in the case of a large centrality dependent modification, as is the case in our model (as well as seen in the experimental data), an unmodified minimum bias R_{dA} is by no means a trivial outcome. This is the first hint that the enhancement in peripheral events is being balanced by the suppression in central events.

The next step is to bin in centrality. Our first attempt will follow convention and utilize the number of binary nucleon-nucleon collisions as an indicator of centrality. One runs the nuclear event generator and collects events, classifying them according to the number of binary collisions. One then bins the event according to where N_{bin} lies in Fig. 4. One should point out that while, on average, an increasing $b(\equiv|\vec{b}|)$ leads to an decrease in N_{bin}, any value of b corresponds to a range of binary collisions. This also modifies the numerator of Eq. (10) to

$$\mathcal{N}_A = \sum_{N_{\mathrm{bin}}} \frac{d^2N_{d\mathrm{Au}}}{d^2p_T dy}\theta\left(N_{\mathrm{bin}} - N_{\mathrm{bin}}^{\min}\right)\theta\left(N_{\mathrm{bin}}^{\max} - N_{\mathrm{bin}}\right), \tag{11}$$

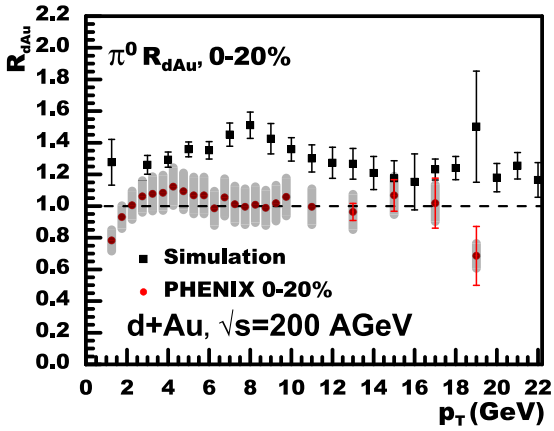

FIG. 13. The nuclear modification factor for neutral pions for 0–20% most central d-Au collisions at RHIC. The simulation is carried out by binning in centrality according to the number of binary collisions (prescription A: see text for details). Simulations include shadowing and no energy loss. Experimental data are taken from Ref. [19]

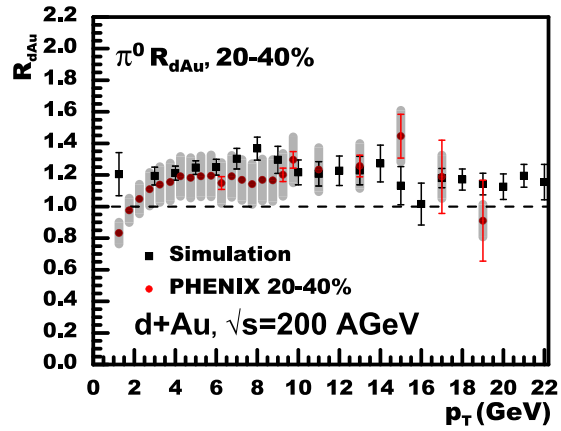

FIG. 14. Same as Fig. 13, except for 20–40% centrality.

where $N_{\rm bin}^{\rm min}$ and $N_{\rm bin}^{\rm max}$ are set by the centrality bin that we are interested in. The factor of $\langle N_{\rm bin}(b_{\rm min}, b_{\rm max})\rangle$ is simply replaced by $\langle N_{\rm bin}\rangle$ for the bin in question, and can be calculated from Fig. 4. This is referred to as prescription A for numerically realizing the numerator of Eq. (10).

An alternate prescription is to classify events according to the number of produced charged particles, utilizing Fig. 11 to divide events into different centrality bins. In this case the numerator is replaced with

$$\mathcal{N}_B = \sum_{N_{\rm ch}} \frac{d^2 N_{d\rm Au}}{d^2 p_T dy} \theta\left(N_{\rm ch} - N_{\rm ch}^{\rm min}\right)\theta\left(N_{\rm ch}^{\rm max} - N_{\rm ch}\right), \quad (12)$$

where $N_{\rm ch}^{\rm min}$ and $N_{\rm ch}^{\rm max}$ are the minimum and maximum values for charged particles produced, set by the centrality bin that we are interested in. The factor of $\langle N_{\rm bin}\rangle$ in the denominator of Eq. (10) now has to be calculated from the collection of events that constitute each centrality bin. We denote this method of calculating the R_{dA} as prescription B.

As most readers are aware, prescription A, is the usual theoretical method of calculating the centrality dependence of the nuclear modification factor, whereas prescription B is closer to the experimental method of determining centrality. We first show the results of simulating the centrality dependence of the pion R_{dA} using prescription A or using the number of binary collisions.

In Fig. 13, the R_{dA} for the top 0–20% most central collisions are plotted. One immediately notes an enhancement in the simulation, but no such enhancement in the experimental data, which seem to be consistent with unity. The simulation does not explain the experimental data. The enhancement in central events, as demonstrated by the simulation, is entirely expected based on the shadowing function that has been used to generate events. Within this framework, the complete lack of any modification in the experimental data is rather surprising; central events should present the maximal nuclear modification.

As one moves up in centrality, from most central to peripheral events, the enhancement seen in the simulation tends to reduce progressively. There is less enhancement in the 20–40% events, even less in the 40–60% simulations, with no modification at all in the 60–88% events, as shown in Figs. 14–16. This behavior of the simulation is entirely expected, as we move from cases with the largest expected nuclear density modification to cases with little density and hence no modification at all in the R_{dA}. The experimental data, however, show an entirely different trend: no modification in the central event and the R_{dA} rising with centrality from most central to most peripheral events. The fact that the simulation results with prescription A match some of those from the experiment is entirely coincidental. The simulation for the R_{dA} drops as one transitions from central to peripheral while the data trend in the opposite direction.

The experimental results for R_{dA} in d-Au collisions are rather unexpected. The largest modification is seen in the most peripheral bin, which by all accounts should resemble p-p most closely. We now attempt to calculate the R_{dA} using prescription B, i.e., using the simulated number of charged particles produced to bin in centrality. The charged particles are gathered over all rapidities, in events that contain a high-p_T π^0, and then compared with the outlined division in Fig. 11.

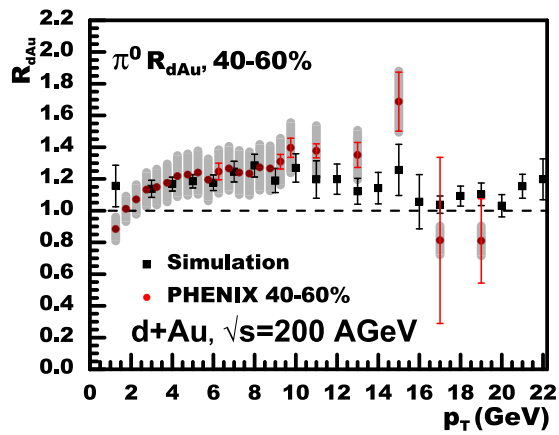

FIG. 15. Same as Fig. 13, except for 40–60% centrality.

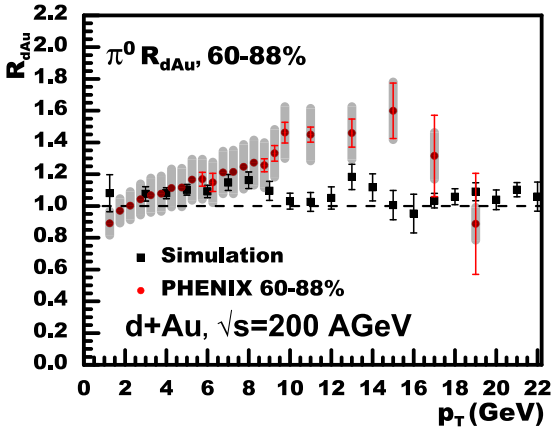

FIG. 16. Same as Fig. 13, except for 60–88% centrality.

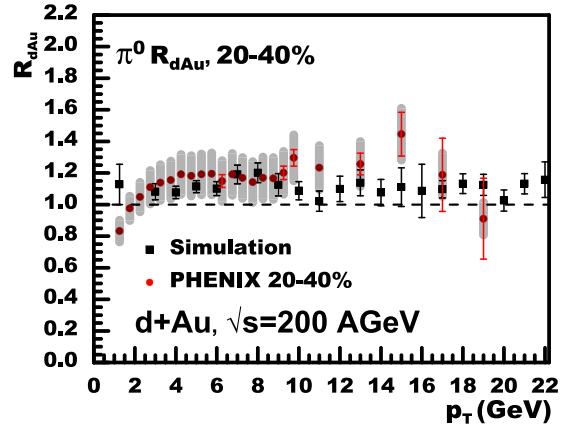

FIG. 18. Same as Fig. 17, except for 20–40% centrality.

Using this prescription, an excellent agreement is obtained with experimental data on the nuclear modification factor of high-p_T neutral pion production as shown in Figs. 17–20. One notes that, for central collisions, the R_{dA} is consistent with 1 and continues to rise as one moves towards more peripheral collisions.

To understand the reason behind the positive comparison between simulation and experiment, we focus on how the events with jets are binned in different centrality bins. In particular we look at how the number of events within each bin change as we transition from binning according to the number of binary collisions to binning according to the number of charged particles produced. We focus on events with a high-p_T pion and isolate the number of events captured in each centrality bin defined by the number of charged particles produced (prescription B), subtracted from the number of events captured in the same bin defined by the number of binary collisions (prescription A). This difference is then expressed as a fraction of the number of events captured using prescription A. This is plotted as a function of the p_T of the pion in Fig. 21. We notice that the number of central and semicentral (20–40%) events, when binned in terms of produced charged particles, are suppressed compared to the case when they are binned according to the number of binary collisions. These lost events show up in the more peripheral collisions, and lead to an enhancement in those collisions. This is the reason that peripheral events as measured in experiment are enhanced compared to binary scaled p-p. Central collisions, compared to binary scaled p-p, are slightly enhanced due to shadowing. These lose events to peripheral collisions and therefore the yield is reduced, leading to the ratio of central collisions to binary scale p-p to be close to unity.

This "movement" of events, from central to less central to peripheral collisions, leads to an enhancement over the expected yield in more peripheral collisions, and a suppression over the expected enhancement in central events. This is mostly an initial state effect. In events with a high-p_T π^0, there has to be a high-x parton in the initial state of at least one nucleon in both the d and the Au nuclei. The presence of a large-x parton in a nucleon of the d depletes the amount of energy available to produce several additional soft partons, and therefore the collisions of this nucleon with nucleons in the Au leads to the

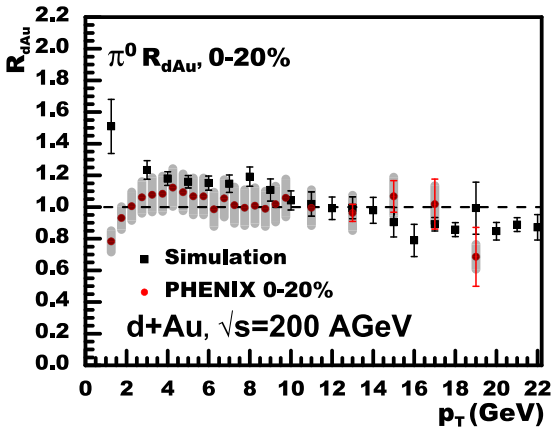

FIG. 17. The nuclear modification factor for neutral pions for 0–20% most central d-Au collisions at RHIC. The simulation is carried out by binning in centrality according to the number of charged particles produced (prescription B: see text for details). Simulations include shadowing and no energy loss. Experimental data are taken from Ref. [19].

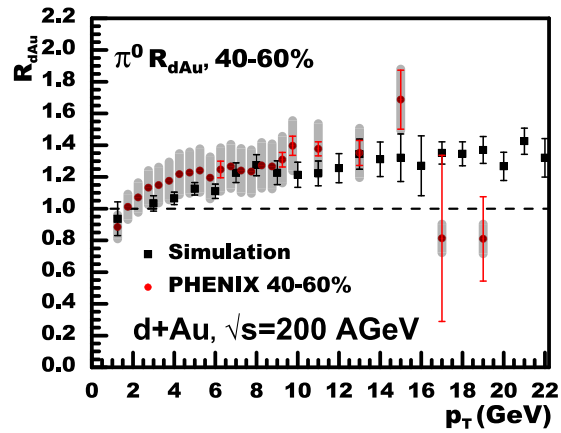

FIG. 19. Same as Fig. 17, except for 40–60% centrality.

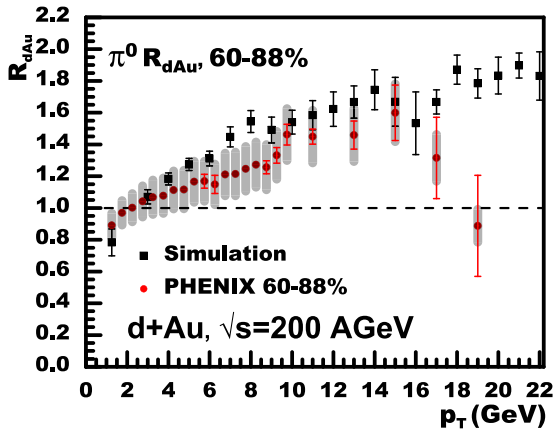

FIG. 20. Same as Fig. 17, except for 60–88% centrality.

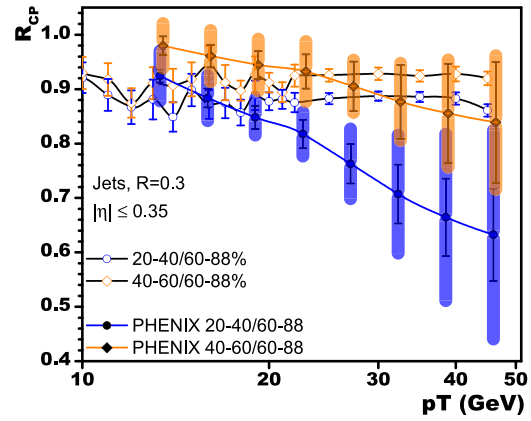

FIG. 22. The ratio of the nuclear modification factor of jets produced in d-Au collisions at RHIC. Experimental data are taken from Ref. [20].

production of fewer charged hadrons. This in turn leads to this event being binned as a more peripheral event.

To test this concept further, we plot the jet R_{CP}, the ratio of the jet spectrum in central to peripheral events, both scaled by the number of expected binary collisions, as a function of p_T in Fig. 22. The results of these simulations are consistent with experimental results if the error bars are considered. There is some concern with the 0–20% central data, as they do not appear to be consistent between jet and pion measurements, therefore they were omitted from the plot. In addition, the differences in the methods to determine centrality (the experimental results were produced by determining centrality by the charge deposited in the Au-going forward detector, whereas our simulation determined centrality by charged particle production over the entire event) as well as in reproducing jets between this simulation and experiment (the jets in the experimental results were reconstructed by applying the anti-k_T algorithm to both electromagnetic clusters and charged particle tracks while rejecting clusters arising from the same particle as a reconstructed track, as stated in Ref. [20]) could account for the observed separation. The R_{CP} is suppressed compared to unity as events move out of more central bins towards more peripheral events. This same effect is transferred via fragmentation to the π^0, and manifests in the R_{dA} as discussed earlier.

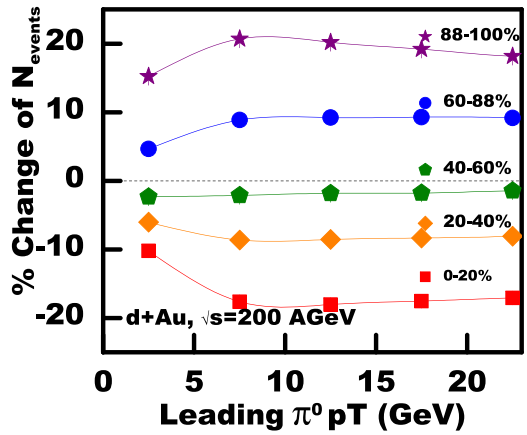

FIG. 21. The fraction of events that shift in or out from each centrality bin as the definition of centrality is changed from binary collisions to number of charged particles produced. The fractional bin shift is plotted as a percentage of the number of events in the original definition with number of binary collisions, as a function of the transverse energy of the detected pion. See text for details.

The primary question at this point is if this effect is solely driven by energy conservation: Is the reduced energy available for the production of small-x partons the only reason for the reduction in the charged particle production, or is there a multiparticle correlation which leads to fluctuation with fewer hard partons, versus fluctuations to several soft partons? In the standard language of pQCD these would be considered as higher-twist multiparton distribution functions. In an alternative formalism, we ask if this is being caused by an initial state *color transparency* [22–24]: the fluctuation of the nucleon to a smaller state with fewer hard partons. In order to study this question further, we consider the modification of this process with the energy of the collision and with the energy of the jet. The higher the energy of the jet, the larger the Q^2 of the process, and, as a result, the smaller the size of the fluctuations will be in the proton. This should lead to a more pronounced effect in similar observables at LHC energies with jets or leading hadrons at much higher energies.

In Fig. 23, we plot the R_{CP} of jets in central p-Pb collisions at mid-rapidity, measured by the ATLAS Collaboration at the LHC. This represents the ratio of the nuclear modification factor in central events (0–10%) to that in peripheral events (60–90%). At high energies, where the effect of energy conservation should become important, our simulation once again compares very well with the data. In Fig. 24, we plot the R_{CP} for charged particles in a similar range of centrality between central and peripheral collisions. In this case, while we obtain the magnitude of the suppression, we do not get the shape of the experimental R_{CP} data. Given that, on the jet side, the agreement between simulation and experiment starts around 60 GeV, the disagreement between the simulation and data for the R_{CP} of charged particles below 100 GeV is somewhat puzzling. It should be pointed out that, in these cases, we are dealing with a larger number of produced partons, all of which

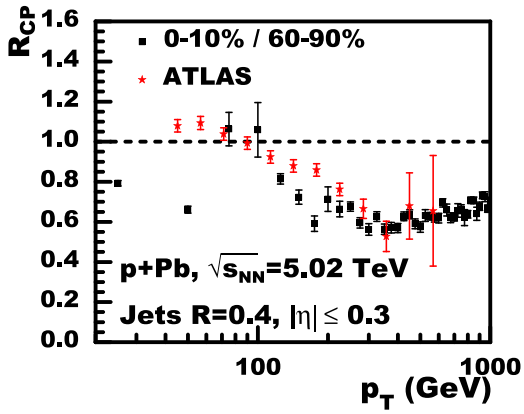

FIG. 23. The ratio of the nuclear modification factor of jets produced in p-Pb collisions at the LHC. Experimental data are taken from Ref. [21].

are color correlated. The effect of this on the fragmentation of the leading parton has not been studied in this effort. The effects of color correlation on jet hadronization have been studied in Ref. [26]. As a result, on the basis of these results, we cannot definitely state whether or not color transparency plays a role in these measurements.

At the risk of repetition, we point out again that our simulations do not in any way contain rescattering and secondary particle production. In the interest of keeping the hard particle production as close to reality as possible (without the need for artificial shadowing), we have abandoned the energy enhanced PDF for the partons in the struck nucleus. There are thus many points of departure between our simulations and the experimental data on soft particle production. Our goal in this effort was to point out that events with a hard jet have a lower soft particle production rate, which leads to binning in a more peripheral bin. While this goal is now firmly established, this work should by no means be considered definitive, as our efforts to determine whether color transparency plays a role in these collisions, beyond energy conservation, has not yielded a clear result. These and other topics will be discussed at length in the subsequent section.

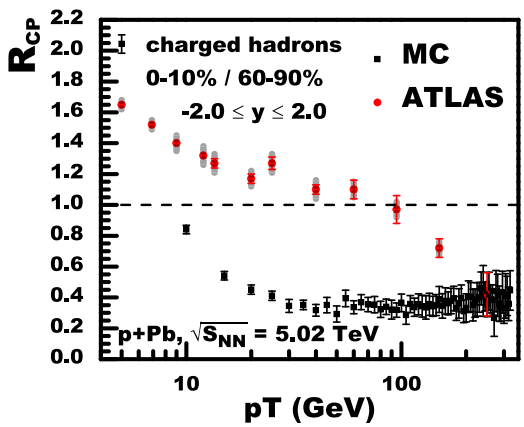

FIG. 24. The ratio of the nuclear modification factor of charged particles produced in p-Pb collisions at the LHC. Experimental data are taken from Ref. [25].

V. DISCUSSION AND OUTLOOK

In this paper, new experimental results from both RHIC and LHC on jet production in extremely asymmetric systems have been discussed. At the energy scales of both RHIC and LHC, similar results were discovered: events that contained a jet or a high energy particle seemed to show an enhancement over binary scaled p-p in peripheral events and a suppression compared to the expectation of shadowing and binary scaling enhanced central collisions. Our goals in this effort were twofold: The first goal was to set up a reliable event generator that could be used to reproduce some portion of the observed experimental data from such collisions. Based on the success of this event generator, our second goal was to determine if the observed behavior can solely be explained by energy conservation or if it requires the incorporation of correlations similar to that of color transparency.

The designed paramete-free event generator consisted of two parts: a nuclear Monte Carlo generator to determine the positions of the nucleons within the nucleus, and a modified version of PYTHIA, with an event-by-event shadowing and PDF enhancement to account for the collision of a nucleon from the $p(d)$ with a column of nucleons within the larger nucleus. The results from these simulations manage to correctly predict the behavior in both the jet R_{CP} and leading particle R_{dA} at RHIC, and the jet R_{CP} at the LHC. The simulation also correctly predicts the magnitude of the suppression in the leading particle R_{CP} at the LHC, though it does not reproduce the shape of the curve. This is a considerable success for such an endeavor. The event generator presented in this effort cannot be considered as complete: there remain several soft observables that, with the given setup of not containing an energy enhanced PDF and without rescattering corrections, cannot be explained. In spite of these, the above study will greatly inform the design of future event generators which will have to be set up to explain these striking experimental data. While this simulation was built on top of the p-p generator PYTHIA, future generators that incorporate all of the above insights will have to be built as a more original effort.

Our goal of setting up the current generator (as well as future generators) was to use it to extract the physics underlying these new observations. These simulations have now established the notion that the enhancement in peripheral events and suppression in central events is entirely due to suppression in soft parton production in a nucleon with a large-x parton. A large portion of this is entirely due to the reduced energy available for soft parton production. Is there any further correlation due to color transparency-like effects? The fact that our Q^2 independent shadowing led to a successful description of the jet R_{CP} at the LHC would seem to rule out such an effect. However, the simulation did not manage to explain the shape of the leading particle R_{CP}. Note that both the leading particle R_{dA} and the jet R_{CP} at RHIC energies were mostly accounted for by the simulation. In order to study such a correlation in greater detail, one needs to devise an event generator which will incorporate an energy enhanced PDF,

with a far more sophisticated shadowing setup to reproduce the large-x behavior of the PDF within a single nucleon. We leave the setup of such an event generator for a future effort. Alternatively, a mechanism will have to be set up where the PDF of the nucleon (or nucleons) from the projectile will have to be sampled once in a $p(d)$-A collision.

Beyond the study of such initial state color transparency effects, a future more advanced event generator for asymmetric collisions such as d-Au or He^3-Au will also allow for a deeper understanding of the quantum correlation between nucleons in a nucleus. In the current work, we have explored excluded volume corrections in a Woods-Saxon distribution, as well as Gaussian perturbations in a shell model based distribution. Experimental data, coupled with theory uncertainties at the partonic level do not allow us to distinguish between the different correlations between nucleons. However, these can be studied systematically, once the partonic component is settled via p-A collisions. This will allow an extension of nuclear structure which has so far not been extensively studied.

Extremely asymmetric nuclear collisions with a hard interaction provide a new window into a large variety of correlation phenomena at multiple scales. Future studies with more accurate experimental data, as well as a more sophisticated event generator, will reveal new information regarding the correlation between partons within a single nucleon, as well as correlations between nucleons in large nuclei. The current work represents a benchmark in this direction, providing a glimpse of the insights that may be gained by such a research program as well as highlighting the ingredients and framework required for future efforts.

ACKNOWLEDGMENTS

The authors would like to thank S. Gavin, G.-Y. Qin and members of the JET Collaboration for helpful discussions. A.M. is indebted to G. David and M. A. Lisa for discussions that led to the genesis of this work. This work was supported in part by the National Science Foundation under Grant No. PHY-1207918, and by the Office of Science of the US Department of Energy under Grant No. DE-SC0013460.

[1] C. Adler *et al.* (STAR Collaboration), Phys. Rev. Lett. **90**, 082302 (2003).
[2] J. Adams *et al.* (STAR Collaboration), Phys. Rev. Lett. **91**, 072304 (2003).
[3] S. S. Adler *et al.* (PHENIX Collaboration), Phys. Rev. Lett. **91**, 072303 (2003).
[4] S. S. Adler *et al.* (PHENIX Collaboration), Phys. Rev. C **75**, 024909 (2007).
[5] S. Adler *et al.* (PHENIX Collaboration), Phys. Rev. Lett. **98**, 172302 (2007).
[6] M. G. Wysocki (PHENIX Collaboration), Nucl. Phys. A **904-905**, 67c (2013).
[7] D. V. Perepelitsa, CERN Technical Report No. ATL-PHYS-PROC-2014-095, CERN, Geneva (2014).
[8] S.-y. Li and X.-N. Wang, Phys. Lett. B **527**, 85 (2002).
[9] T. Sjöstrand, S. Ask, J. R. Christiansen, R. Corke, N. Desai, P. Ilten, S. Mrenna, S. Prestel, C. O. Rasmussen, and P. Z. Skands, Comput. Phys. Commun. **191**, 159 (2015).
[10] A. Bzdak, V. Skokov, and S. Bathe, Phys. Rev. C **93**, 044901 (2016).
[11] M. Alvioli, B. A. Cole, L. Frankfurt, D. V. Perepelitsa, and M. Strikman, Phys. Rev. C **93**, 011902 (2016).
[12] N. Armesto, D. C. Gülhan, and J. G. Milhano, Phys. Lett. B **747**, 441 (2015).
[13] X.-N. Wang and M. Gyulassy, Phys. Rev. D **44**, 3501 (1991).
[14] M. Gyulassy and X.-N. Wang, Comput. Phys. Commun. **83**, 307 (1994).
[15] W. Greiner and J. A. Maruhn, *Nuclear Models* (Springer, Berlin, 1996).
[16] A. Majumder and S. Das Gupta, Phys. Rev. C **59**, 845 (1999).
[17] P. Brussaard and P. Glaudemans, *Shell Model Applications in Nuclear Spectroscopy* (Elsevier, Amsterdam, 1977).
[18] T. Sjostrand and M. van Zijl, Phys. Rev. D **36**, 2019 (1987).
[19] B. Sahlmueller (PHENIX Collaboration), Nucl. Phys. A **904-905**, 795c (2013).
[20] A. Adare *et al.*, Phys. Rev. Lett. **116**, 122301 (2016).
[21] G. Aad *et al.* (ATLAS Collaboration), Phys. Lett. B **748**, 392 (2015).
[22] S. J. Brodsky, L. Frankfurt, J. F. Gunion, A. H. Mueller, and M. Strikman, Phys. Rev. D **50**, 3134 (1994).
[23] L. Frankfurt, G. A. Miller, and M. Strikman, Phys. Lett. B **304**, 1 (1993).
[24] L. L. Frankfurt and M. I. Strikman, Phys. Rep. **160**, 235 (1988).
[25] ATLAS Collaboration, Report No. ATLAS-CONF-2014-029, CERN, Geneva (2014).
[26] A. Beraudo, J. G. Milhano, and U. A. Wiedemann, Phys. Rev. C **85**, 031901 (2012).